Limit-cycle oscillations and stable patterns in repressor lattices

Sagar Chakraborty,[1,*] Mogens H. Jensen,[2,†] Sandeep Krishna,[3,‡] Benedicte Mengel Pers,[2,§] Simone Pigolotti,[4,‖] Vedran Sekara,[2,¶] and Szabolcs Semsey[2,**]

[1]*NBIA, Niels Bohr Institute, University of Copenhagen, Blegdamsvej 17, 2100 Copenhagen Ø, Denmark*

[2]*CMOL, Niels Bohr Institute, University of Copenhagen, Blegdamsvej 17, 2100 Copenhagen Ø, Denmark*

[3]*NCBS, Tata Institute of Fundamental Research, GKVK Bellary Road, Bangalore 560065, India*

[4]*Dept. de Fisica i Eng. Nuclear, Universitat Politecnica de Catalunya, Edif. GAIA, Rambla Sant Nebridi s/n, 08222 Terrassa, Barcelona, Spain*

(Received 3 February 2012; revised manuscript received 6 July 2012; published 7 September 2012)

As a model for cell-to-cell communication in biological tissues, we construct repressor lattices by repeating a regulatory three-node motif on a hexagonal structure. Local interactions can be unidirectional, where a node either represses or activates a neighbor that does not communicate backwards. Alternatively, they can be bidirectional where two neighboring nodes communicate with each other. In the unidirectional case, we perform stability analyses for the transitions from stationary to oscillating states in lattices with different regulatory units. In the bidirectional case, we investigate transitions from oscillating states to ordered patterns generated by local switches. Finally, we show how such stable patterns in two-dimensional lattices can be generalized to three-dimensional systems.

DOI: 10.1103/PhysRevE.86.031905 PACS number(s): 87.18.Hf, 05.45.−a

I. INTRODUCTION

Biological systems are in general composed of many interacting units. On the cellular level, proteins, ribonucleic acid (RNA), small molecules, and genes interact through a complex regulatory system. On the level of tissues, cells interact with each other through gap junctions or through diffusible or cell-surface bound signaling molecules. On the organism level, even more complex interactions take place. It is thus of fundamental importance to investigate how smaller units of regulatory systems interact with each other [1]. Recently a way to couple regulatory units each consisting of three nodes on a hexagonal lattice have been introduced [2], as a generalization in space of the *repressilator* [3]. In the latter model, three proteins repress each other by blocking the associated genes. Depending on the parameters, such a circuit can generate either a stationary state, where the protein concentrations remain constant, or a dynamically varying state where the concentrations oscillate as time progresses. By introducing a constructed plasmid into *E. coli,* such oscillations were also observed in a genetically manipulated system [3]. Previously other papers have studied coupled repressilators to investigate quorum sensing [4] and to describe cell-to-cell communication [5]. Repressilator motifs placed on a hexagonal lattice, where nodes now can be viewed as cells in an interacting tissue, constitute an intriguing system where the activity of each cell can oscillate out of phase with its neighbors in a completely regular fashion [2]. Surprisingly, such oscillating states can evolve dynamically unfrustrated (in the sense explained in the next section) even in a tissue of infinite size. This is particularly interesting in view of the fact that hexagonal ordering is often found in cells composing tissues such as hepatic or retinal [6–8]. This happens especially in planar tissues because of close packing of cells.

In many tissues, neighboring cells interact directly (juxtacrine signaling) through bidirected interactions (e.g., using gap junctions or membrane-bound signaling molecules). In these systems each cell can regulate its neighbors laterally. The best studied model system of juxtacrine signaling is the Delta-Notch system, which is present in many multicellular organisms [9–12]. Using Delta-Notch signaling, cells express a signal that can influence the gene expression pattern of neighboring cells. This mechanism results in two distinct differentiation pathways in the initially equivalent cells, allowing formation of fine-grained patterns in large structures.

The example of Delta-Notch signaling inspired the study of patterns in lateral inhibition models [13–17]. These models can be viewed as simplified versions of the juxtacrine signaling systems, in which the circuit inside each cell is reduced to a single protein concentration, whose effect is to inhibit the production of the same protein in neighboring cells. It has been shown [15] that these models generically lead to regular patterns where the expression activity in each cell can be up or down, and on each row a repeated up-down-down pattern is found, so that each cell with a high activity is surrounded by silenced cells.

When the lateral inhibition is symmetric, oscillating states are ruled out. Instead, the system effectively consists of local switches where each cell will be either in an active (high) or a silenced (low) state. Reference [18] studied how such a tissue grows during cell divisions and migrations. In general the tissue settles into ordered states where the silenced and the active cells are arranged in regular patterns. Under certain growth conditions, however, it was found that areas of disordered patterns might appear [18].

In this paper, following the results of Refs. [2,18], we perform a theoretical analysis of the repressor lattice. Furthermore, we introduce regulating lattices where activators and repressors alternate in an orderly fashion. Of course, the claim of unidirectional feedback between similar cells in

*sagar@nbi.dk
†mjensen@nbi.dk
‡sandeep@ncbs.res.in
§bmengel@nbi.dk
‖simone.pigolotti@upc.edu
¶vedran@fys.ku.dk
**semsey@nbi.dk

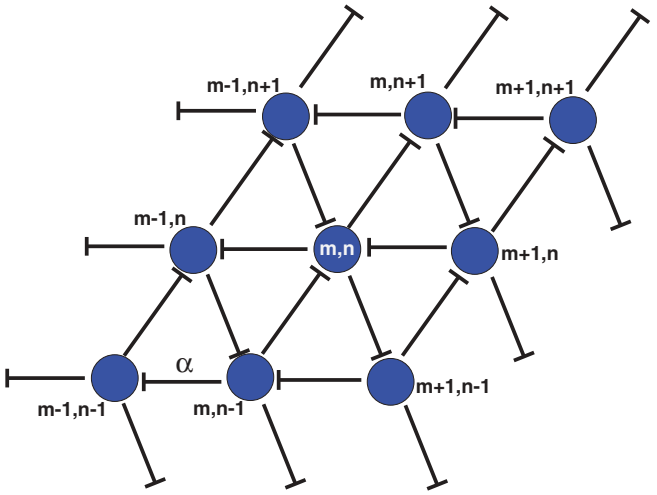

FIG. 1. (Color online) Unidirectional interaction: Scheme of the directed interaction in a repressor lattice.

a tissue is rather unrealistic, and hence, we also take into account bidirectional feedback in this paper. To this end, we study a bidirectional repressor lattice with asymmetric coupling between the cells, which leads to a transition between oscillating and stationary states. Furthermore, since most of the tissues naturally occur with a three-dimensional (3D) arrangement of the constituent cells, we generalize the two-dimensional (2D) repressor lattice in three dimensions and discuss the possible patterns in the higher dimensions.

II. THE REPRESSOR LATTICE

In this section we briefly study the periodic repressor lattice along the lines of the results obtained in Ref. [2]. We consider a triangular lattice with directed interaction as in Fig. 1. The variables $x_{m,n}$ represent concentrations or activities of the regulatory proteins at coordinate (m,n) in the lattice. We assume that the neighboring cells interact with each other in accordance with the following set of dynamical equations:

$$\frac{dx_{m,n}}{dt} = c - \gamma x_{m,n} + \alpha F_{\rm int}; \quad m,n \in \{1,2,\ldots,L\}, \tag{1}$$

where the interaction term $F_{\rm int}$ is of the form

$$F_{\rm int} = \frac{1}{1+\left(\frac{x_{m+1,n}}{K}\right)^h} + \frac{1}{1+\left(\frac{x_{m,n-1}}{K}\right)^h} + \frac{1}{1+\left(\frac{x_{m-1,n+1}}{K}\right)^h}, \tag{2}$$

and L is the periodicity of the lattice. Expression (2) assumes that the effects of different inhibition of each cell are additive. However, it is worth to remark that one can find similar dynamics in the case of *multiplicative* interactions such as

$$F_{\rm int} = \frac{1}{1+\left(\frac{x_{m+1,n}}{K}\right)^h} \times \frac{1}{1+\left(\frac{x_{m,n-1}}{K}\right)^h} \times \frac{1}{1+\left(\frac{x_{m-1,n+1}}{K}\right)^h}. \tag{3}$$

In both cases (2) and (3), the repression is modeled via standard Michaelis-Menten terms. The parameters c, γ, and α, respectively, measure the constitutive production of the proteins, the degradation rate, and the strength of the repression by another protein. Further, K is the dissociation constant of the binding complex whose cooperativity is measured by the parameter h, the Hill coefficient. For the sake of simplicity, we have assigned the same parameter values to all the nodes in the lattice.

To investigate the dynamics of the system (1), we first search for an homogeneous solution:

$$x_{m,n} = x^* \,\forall m,n \;\longrightarrow\; 3\alpha K^h = (\gamma x^* - c)(K^h + x^{*h}). \tag{4}$$

It is straightforward to show (e.g., by graphical methods) that this solution exists and is unique. We then consider a perturbation of this solution in form of a plane wave, $x_{m,n}(t) = x^* + \epsilon \exp[\lambda t + 2\pi i(k_m m + k_n n)/L]$. Plugging this solution into (1) and neglecting terms of order higher than ϵ yields the following dispersion relation:

$$\lambda = -\tilde{a} f(k_m,k_n) - \gamma \tag{5}$$

with $\tilde{a} \equiv \alpha h K^h x^{*(h-1)}/(K^h + x^{*h})^2$ and

$$f(k_m,k_n) \equiv e^{\frac{2\pi i k_m}{L}} + e^{-\frac{2\pi i k_n}{L}} + e^{\frac{2\pi i (k_n - k_m)}{L}}. \tag{6}$$

It is convenient to rescale the wave numbers by defining $\tilde{k}_m \equiv k_m/L$ and $\tilde{k}_n \equiv k_n/L$ and by studying the function $g(\tilde{k}_m,\tilde{k}_n) \equiv e^{2\pi i \tilde{k}_m} + e^{-2\pi i \tilde{k}_n} + e^{2\pi i(\tilde{k}_n - \tilde{k}_m)}$. Since wave functions should have the same periodicity of the lattice, the entries of the vectors k_m and k_n are integer numbers between 1 and L (both numbers inclusive). This means that $\tilde{k}_m\, \tilde{k}_n \in (0,1]$ and $\tilde{k}_m$, $\tilde{k}_n$ should be of the form j/L with j being an integer.

We now look for the global minimum of the real part of g. From Eq. (5), one can conclude that if such a minimum is larger than $-\gamma/\tilde{a}$, the homogeneous state is unstable, and the eigenfunctions corresponding to the minimum eigenvalue are the most unstable modes. The function g achieves its global minima at $g(1/3,2/3) = g(2/3,1/3) = -3/2$. It is easy to show that these two eigenfunctions correspond to a complex conjugate pair of eigenvalues, implying that the destabilization of the homogeneous solution occurs via a Hopf bifurcation. Moreover, both eigenfunction are invariant for rotations of $2\pi/3$ and $4\pi/3$; i.e., they preserve all the symmetries of the lattice. The corresponding oscillations may be considered as an extension to the whole lattice of the basic solution of the repressilator circuit [3], with three different phases. Numerical investigation (see Ref. [2]) shows that this solution remains stable even far from the Hopf bifurcation; i.e., no further symmetries are broken when α is increased.

The wave functions corresponding to the minimum of g, however, cannot be obtained when L is not a multiple of three because of the boundary conditions. In these cases we have to search for global minima of the real part of g among the allowed wave functions. In general, these functions are not invariant under rotations of $2\pi/3$ and $4\pi/3$, so that we expect three different complex conjugate pairs of eigenvalues to cause the Hopf bifurcation. Since there is a limited number $L \times L$ of eigenfunctions, the minimum solutions for each L may be found by exhaustive search. For $L = 4$, we have six degenerate minima: (1/4, 2/4), (2/4, 1/4), (1/4, 3/4), (3/4, 1/4), (2/4, 3/4), and (3/4, 2/4). For $L = 5$, the solutions are six: *viz.*, (1/5, 3/5), (3/5, 1/5), (2/5, 3/5), (3/5, 2/5), (2/5, 4/5), and (4/5, 2/5).

The broken rotational symmetry for L, not a multiple of three, influences the behavior of the system also far from the Hopf bifurcation. Depending on L, increasing α farther may

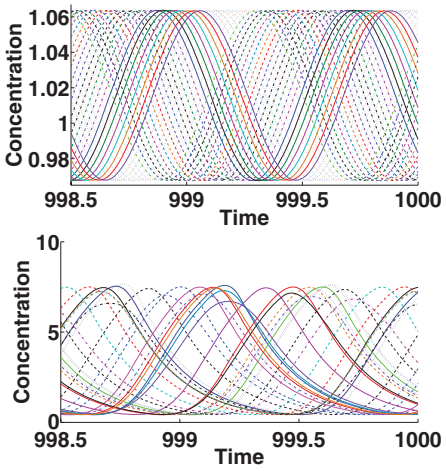

FIG. 2. (Color online) Dynamics of the system for $L = 31$. While $\gamma = 4.4, K = 1, c = 0.1$, and $h = 4$ are same for both the figures above, $\alpha = 3$ and 15, respectively, for the upper and the lower panels.

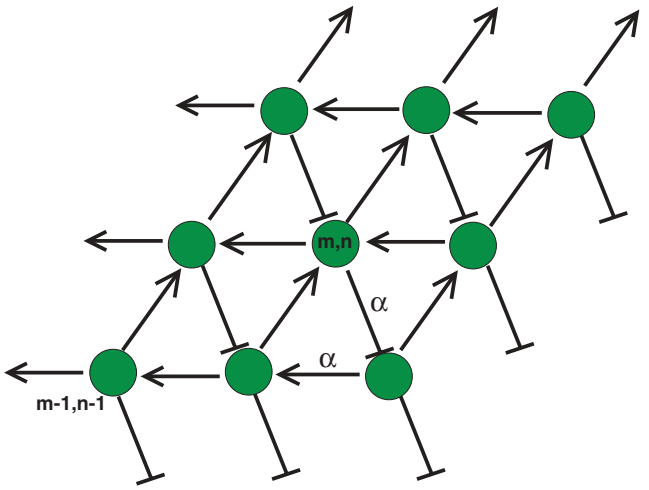

FIG. 3. (Color online) Scheme of the directed unidirectional mixed type interaction in an activator-activator-repressor lattice. Lines with arrowheads indicate activation.

result in the solutions breaking also the translational symmetry of the lattice. For $L = 5$, we also observed a transition to chaos [2]. When L becomes larger and larger (without being a multiple of three) the number of eigenfunctions increases, so that it becomes easier to obtain a minimum of the real part of g being very close to the absolute minimum.

However, the possibility of breaking other symmetries persists, suggesting that it is not a peculiarity of small circuits. We interpret this result as a frustration effect: Even if the minimum is well approximated, the eigenfunction cannot be a periodic repetition of the basic repressilator motif because of the mismatch imposed by the boundary conditions [2]. Figure 2 shows an example with $L = 31$. The upper panel is just past the Hopf bifurcation, where 31 distinct and equispaced phases are observed through the lattice. The lower panel shows the dynamics when α is increased well beyond the threshold value at the Hopf bifurcation, so that translational symmetry is broken and the phases become irregular. For higher values of α, the lattice starts showing chaotic behavior which becomes more and more prominent as α is raised further. That the lattice exhibit chaos can be validated by the fact that the maximum Lyapunov exponent is positive; e.g., for the case $\alpha = 20$, it is 6.7×10^{-4}.

III. ACTIVATOR-ACTIVATOR-REPRESSOR LATTICES

Most biological oscillations are caused by a negative feedback loop composed by both activators and repressors, the simplest being a loop of two proteins A and B, such that A activates B and B represses A. We explore in this section the result of generalizing such a circuit to a lattice. We shall find that the heterogeneity of the interactions leads to more complex oscillations than in the case discussed in the previous section, where all interactions are repressions.

We focus on the triangular lattice as shown in Fig. 3. This lattice has directed interactions; however, this time not all the interactions are repressing: Some are activating. We model the concentration $x_{m,n}$ of, say, a protein at a (m,n) cell by the following ordinary differential equation:

$$\frac{dx_{m,n}}{dt} = c - \gamma x_{m,n} + \alpha F_{\rm int}^{(a)} + \beta F_{\rm int}^{(r)}, \tag{7}$$

where the interaction terms due to the activators and the repressors are, respectively, of the form

$$F_{\rm int}^{(a)} = \frac{\left(\frac{x_{m+1,n}}{K}\right)^h}{1+\left(\frac{x_{m+1,n}}{K}\right)^h} + \frac{\left(\frac{x_{m,n-1}}{K}\right)^h}{1+\left(\frac{x_{m,n-1}}{K}\right)^h}, \tag{8}$$

$$F_{\rm int}^{(r)} = \frac{1}{1+\left(\frac{x_{m-1,n+1}}{K}\right)^h}. \tag{9}$$

For simplicity, we fix $\beta = \alpha$. Of course, α in this section should not be confused with the α defined in earlier sections. As usual, we search for an homogeneous solution: $x_{m,n} = x^* \; \forall m,n$, that satisfy

$$\gamma x^{*(h+1)} - (c+2\alpha)x^{*h} + \gamma K^h x^* - (c+\alpha)K^h = 0. \tag{10}$$

We consider perturbations of this solution of the form $x_{m,n}(t) = x^* + \epsilon \exp[\lambda t + 2\pi i(k_m m + k_n n)/L]$. Substituting into Eq. (7) yields the following dispersion relation:

$$\lambda = \tilde{a} f(k_m,k_n) - \gamma + O(\epsilon^2), \tag{11}$$

with $\tilde{a} \equiv \alpha h K^h x^{*(h-1)}/(K^h + x^{*h})^2$ and

$$f(k_m,k_n) \equiv e^{\frac{2\pi i k_m}{L}} + e^{-\frac{2\pi i k_n}{L}} - e^{\frac{2\pi i (k_n - k_m)}{L}}. \tag{12}$$

Note while there is a negative sign associated with the first term in the right-hand side of Eq. (5), we have a positive sign in the similar place in Eq. (11). This is also the reason why we shall consider global maxima in what follows rather than the global minima as has been done in the earlier section. For the sake of convenience, we define

$$g(\tilde{k}_m,\tilde{k}_n) \equiv e^{2\pi i \tilde{k}_m} + e^{-2\pi i \tilde{k}_n} - e^{2\pi i(\tilde{k}_n - \tilde{k}_m)}, \tag{13}$$

where $\tilde{k}_m$ and $\tilde{k}_n$ are the components of the discrete wave vector divided by L. It may be noted that, as shown in Fig. 4, the global maxima of real part of g correspond to the points $(1/6, 5/6)$ and $(5/6, 1/6)$. $g(\tilde{k}_m,\tilde{k}_n) = 3/2$ at global maxima. These maxima

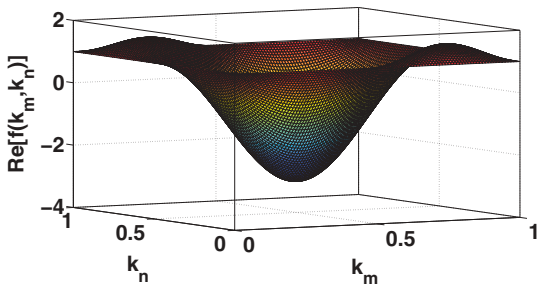

FIG. 4. (Color online) Dispersion relation of the activator-activator-repressor model.

are realized for $L = 6$ and its multiples. Depending on the values of $\tilde{a}$ and γ, the corresponding complex eigenvalues can have positive real part resulting in destabilization of the homogenous solution via Hopf bifurcation. One can numerically solve the dynamical equation (7) for the parameter values $\alpha = 3.0, \gamma = 4.7, K = 1, c = 0.1$, and $h = 4$ to find oscillations just past the Hopf bifurcation. The resulting oscillations have six distinct equispaced phases. One also encounters Hopf bifurcation for $L \neq 6$ for carefully chosen parameters. It is, however, worth emphasizing that for lattices of size $L \times L$, with $L \neq 6$ (or its multiples), there exists no maxima of the kind mentioned above for $L = 6$. This is simply because $(\tilde{k}_m, \tilde{k}_n) = (k_m/L, k_n/L)$, in definition (13), can be only $(1/6, 5/6)$ or $(5/6, 1/6)$ for the global maxima in question; and so if $L \neq 6N$ (N being a natural number), one cannot find natural numbers k_m and k_n which will satisfy the required condition. Recall that k_m and k_n must be natural numbers between 1 and L (both numbers inclusive) as $x_{m,n}(t)$ must have the periodicity of the lattice.

With a view to comparing how heterogeneity of interaction causes the system to behave differently than a pure repressor lattice, in Fig. 5, we have plotted the total number of distinct phases that an $L \times L$ activator-activator-repressor lattice yields just past the Hopf bifurcation and compared it with the total number of distinct phases that an $L \times L$ repressor lattice yields just past the Hopf bifurcation. While we have discussed the phases of oscillations in repressor lattice in the preceding section, let us discuss briefly the number of phases of oscillations vis-à-vis lattice size in the activator-activator-repressor lattice. For $L = 6N$, number of distinct phases is always six. Recall that the part of the argument of cosine that is responsible for the different phases in

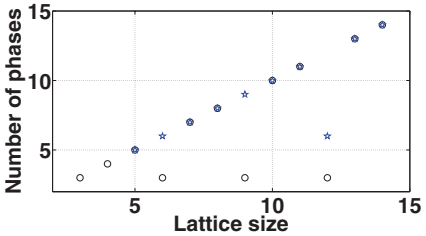

FIG. 5. (Color online) Numerically validated number of different phases as a function of L for the repressor-lattice (circles) and the activator-activator-repressor lattice (stars). We were unable to numerically find any limiting oscillatory state for the activator-activator-repressor lattice when $L = 3$ and 4.

the solutions $x_{m,n}(t) = x^* + \epsilon \exp[\lambda t + 2\pi i(k_m m + k_n n)/L]$ is $\phi \equiv 2\pi(k_m m + k_n n)/L$. For all possible nodes (m,n), it is easily seen that, within a factor of an integral multiple of 2π, ϕ can have only six distinct values when $L = 6N$, which requires $(k_m/L, k_n/L)$ to be equal to $(1/6, 5/6)$ or $(5/6, 1/6)$ for the most unstable mode.

When $L \neq 6N$, we know that there can be no maxima for $f(k_m, k_n)$ in Eq. (12). However, one can still find k_m, k_n such that λ in Eq. (11) becomes positive; e.g., for $L = 8$, the maximum value of $f(k_m, k_n) = 1.4142$ occurs *degenerately* for $(\tilde{k}_m, \tilde{k}_n) = (k_m/L, k_n/L) = (1/8, 7/8)$ [or $(7/8, 1/8)$] and also for $(1/8, 6/8)$ [or $(6/8, 1/8)$]. One can readily see that ϕ (modulo 2π) in this case will have eight distinct values. This argument runs through for all other L, and one thus expects that number of distinct phases to be equal to the lattice size L except when $L = 6N$ $(N \geqslant 2)$ in which case the number of distinct phases is always six owing to the existence of global maxima for $f(k_m, k_n)$. This is exactly what has been validated in Fig. 5 generated from simulations.

However, one may note the absence of data points for $L = 3, 4$ in Fig. 5. It is because we were unable to find the right set of parameters. What we mean is the following: When one tries to find a "right set of parameters" which will make λ in Eq. (11) positive, leading to oscillatory solutions via Hopf bifurcation, one has to keep it in mind that this equation is coupled to Eq. (10) (through $\tilde{a}$), which is not easy to solve analytically for arbitrary values of the parameters. Probably the best one can do is to try and scan the parameter space numerically in search of parameters that make λ positive. Unfortunately, even after an extensive search, we could not find the right set of parameters; moreover, we were unable to argue either absence or presence of such a set of parameters analytically. Hence the last word on whether the activator-activator-repressor lattice has oscillatory solutions for $L = 3, 4$ is still to come.

IV. BIDIRECTIONAL INTERACTIONS

The repressor lattice of Ref. [2] would require a planar array of cells in which each unit represses three other cells and is repressed by other three. While directional cell-to-cell communication has been observed, the assumption of the perfect directional communication is quite strong and unlikely to be the case in a real biological system. On the other hand, a completely symmetric communication system would not show any oscillatory dynamic behavior because the characteristic matrix, found upon linearization, is real symmetric, allowing only real eigenvalues.

A. Oscillations for asymmetrical interactions

In this subsection we examine intermediate situations of nonperfect directed interactions. In particular, for each directed interaction of the original model, having an intensity α_1, we assume the opposite interaction also to occur, with an intensity α_2 such that $\alpha_2 < \alpha_1$, as represented in Fig. 6.

The equation describing the model is

$$\frac{dx_{m,n}}{dt} = c - \gamma x_{m,n} + \alpha_1 F_{\text{int}} + \alpha_2 F'_{\text{int}} \qquad (14)$$

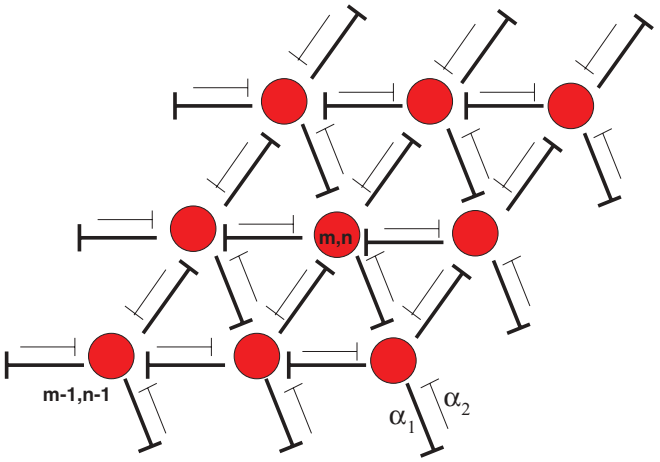

FIG. 6. (Color online) Bidirectional interaction: Scheme of the nonperfect or asymmetrical directed interaction. The thinner repressing arrows represent the backward interactions.

with

$$F_{\text{int}} \equiv \frac{1}{1+\left(\frac{x_{m-1,n+1}}{K}\right)^h} + \frac{1}{1+\left(\frac{x_{m,n-1}}{K}\right)^h} + \frac{1}{1+\left(\frac{x_{m+1,n}}{K}\right)^h}, \tag{15}$$

$$F'_{\text{int}} \equiv \frac{1}{1+\left(\frac{x_{m-1,n}}{K}\right)^h} + \frac{1}{1+\left(\frac{x_{m,n+1}}{K}\right)^h} + \frac{1}{1+\left(\frac{x_{m+1,n-1}}{K}\right)^h}. \tag{16}$$

We would like to understand if the oscillations observed in the unidirectional lattice are robust to the introduction of the backward interaction.

It is easy to seek a homogeneous solution. In fact, the fixed point condition turns out to be exactly the same as Eq. (4), with α replaced by $(\alpha_1+\alpha_2)$. Performing a stability analysis about this constant solution leads us to

$$\lambda = -\tilde{a}_1 f(k_m,k_n) - \tilde{a}_2 \overline{f(k_m,k_n)} - \gamma, \tag{17}$$

when the bar denotes complex conjugation and the definition of $\tilde{a}_1$, $\tilde{a}_2$ are parallel with those of the previous section. For convenience, we separate the real and imaginary part of the dispersion relation

$$\begin{aligned}\lambda = &\{-\gamma - (\tilde{a}_1+\tilde{a}_2)\text{Re}[f(k_m,k_n)]\} \\ &+ i\{(\tilde{a}_2-\tilde{a}_1)\text{Im}[f(k_m,k_n)]\}.\end{aligned} \tag{18}$$

Consider a directed system of the form (1) and a bidirectional of the form (14), chosen such that $\alpha = (\alpha_1+\alpha_2)$. According to the analysis above, they will have the same homogeneous solution. Moreover, the real part of their eigenvalues will be the same, meaning that their homogenous solutions will be either both stable or both unstable. Also in the bidirectional case, the transition will occur via a Hopf bifurcation. The only exception is the special case in which one has perfect bidirectionality, $\alpha_1 = \alpha_2$, where the stability matrix is symmetric; and thus, all the eigenvalues are real, and any oscillation is ruled out.

To check the dependence on the degree of asymmetry of the interactions, we fix α_1 and α_2 in such a way that the system is just past the Hopf bifurcation and start varying their difference $\alpha_1 - \alpha_2$. According to Hopf theorem, the period of the oscillations at the transition point is $2\pi/|\tilde{a}_1 - \tilde{a}_2|$. This means that the only effect of increasing the symmetry of the interaction, with $\alpha_1+\alpha_2$ fixed, is to increase the period of the oscillations. In particular, the period diverges as the system becomes more and more symmetric. In Fig. 7 we investigate the system and find the aforementioned expected behavior.

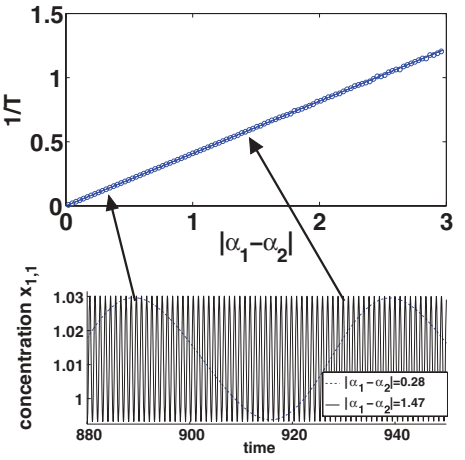

FIG. 7. (Color online) Inverse of the period as a function of the asymmetry $|\alpha_1 - \alpha_2|$. The theoretical solid straight line is in excellent agreement with the simulation's results (blue circles). Two time series are shown as examples. $\alpha_1+\alpha_2 = 2.99, \gamma = 4.43$, $K = 1, c = 0.1, h = 4$.

B. Ordered patterns for symmetrical interactions

In this subsection we shall restrict ourselves to the case of the symmetrical interactions meaning $\alpha_1 = \alpha_2 = \alpha$, not to be confused with α introduced in earlier sections. It has been shown in a very recent work [18], based on governing equations involving multiplicative bidirectional repression of Michaelis-Menten type, that very robust (immune to mutations) ordered patterns are produced during tissue growth via cell division or migration. Their work has been done for a finite extent of tissue with "open" boundaries. Here we want

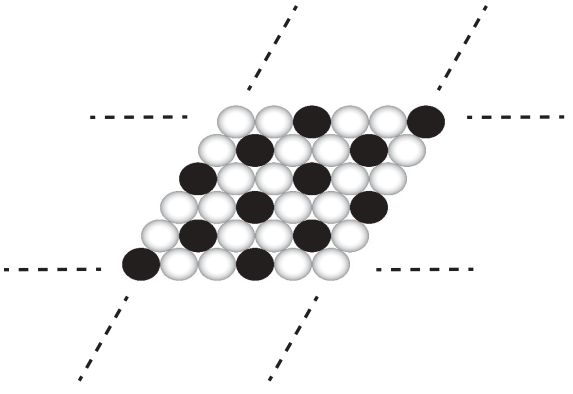

FIG. 8. The black cells have higher concentration than the white cells in the high-low-low (HLL) pattern, while just the opposite happens in the low-high-high (LHH) pattern. In the homogeneous ($\mathcal{H}$) pattern, the black and the white cells have the same concentrations.

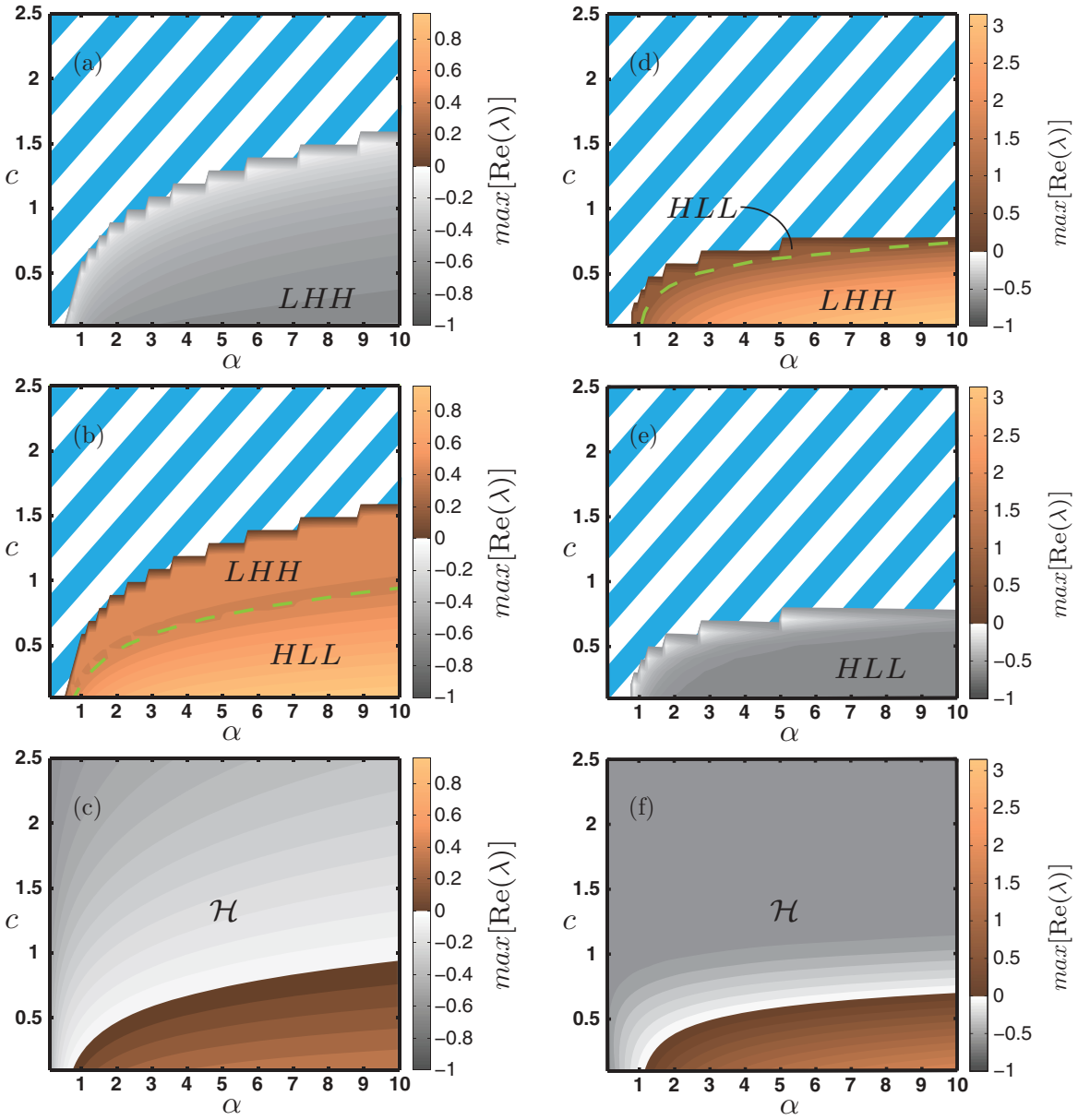

FIG. 9. (Color online) Plots with tags (a), (b), and (c) are for additive bidirectional interactions while plots (d), (e), and (f) are for multiplicative bidirectional repressions. Plots (a), (b), and (c), respectively, show the maxima of the real parts of the eigenvalues (max[Re(λ)]) determining stability of the fixed points (x^*, y^*) corresponding to the LHH, the HLL, and the $\mathcal{H}$ patterns. The dashed green line in plot (b) is the boundary between the HLL and the LHH patterns in the parameter space of c and α. The HLL appearing adjacent to the green dashed line in plot (b) should not be confused with the HLL patterns appearing in plot (a) for the same c and α values. Appearance of the two different HLL patterns for the same parameter values, as can be seen by comparing plots (a) and (b), indicates that while for some parameter values there are three positive solutions $(x^* > 0, y^* > 0)$ to Eq. (19), none of them corresponds to the LHH pattern. The cyan-white cross-striped regions depict the ranges of parameter space where the corresponding fixed point solutions (and hence the related pattern whether stable or unstable) are nonexistent. Plots (d), (e), and (f) should be understood along the line discussed above. For all plots, $\gamma = 1$, $K = 1$, and $h = 3$.

to focus on a 3×3 periodic bidirectionally interacting cells' lattice, wherein oscillations are not possible owing to assumed symmetry of interactions, and we want to study simple ordered patterns that are possible for both the additive as well as the multiplicative interactions.

One can easily figure out, by looking at the inherent symmetry of the lattice shown in Fig. 6, that the simplest possible pattern is the case when all the cells have the same value for $x_{m,n}$. We shall call this pattern *homogeneous* ($\mathcal{H}$) for obvious reasons. The next stage in the hierarchy of possible ordered patterns are the patterns wherein any cell can have one of two different values for $x_{m,n}$. Assuming that there are two such values for $x_{m,n}$, one being higher than the other, the two possible patterns would be (1) the central cell in Fig. 6

has the *high* value and is surrounded by six other cells having the *low* values and (2) the central cell has the low value and is surrounded by six other cells having the high values. We shall call these two patterns *high-low-low* (HLL) and *low-high-high* (LHH), respectively (see Fig. 8).

In order to mathematically study the HLL and the LHH patterns, we let x^* denote either one of the high value or the low value after equilibrium is reached and y^* denote the other value. x^* and y^* will obey the following set of equations for additive and multiplicative interactions, respectively:

$$c - \gamma x^* + \frac{6\alpha}{1 + \left(\frac{y^*}{K}\right)^h} = 0, \tag{19a}$$

$$c - \gamma y^* + \frac{3\alpha}{1 + \left(\frac{x^*}{K}\right)^h} + \frac{3\alpha}{1 + \left(\frac{y^*}{K}\right)^h} = 0, \tag{19b}$$

and

$$c - \gamma x^* + \alpha \left[\frac{1}{1 + \left(\frac{y^*}{K}\right)^h}\right]^6 = 0, \tag{20a}$$

$$c - \gamma y^* + \alpha \left[\frac{1}{1 + \left(\frac{x^*}{K}\right)^h}\right]^3 \left[\frac{1}{1 + \left(\frac{y^*}{K}\right)^h}\right]^3 = 0. \tag{20b}$$

To render the above mathematical picture more clear, we may remark that x^* used above is a *fixed point* value of $x_{m,n}$ for the central cell in Fig. 6. It is not easy to obtain closed analytical form of solutions for x^* and y^* from Eqs. (19) and (20), so we proceed to study them numerically. We can always rescale time t and $x_{m,n}$ such that two parameters, γ and K (say), are unity, and we can redefine remaining parameters. Under the constraint that $x^*, y^* > 0$, we find that in the most general case, both sets of Eqs. (19) and (20) have three simultaneous solutions representing the $\mathcal{H}$, the HLL, and the LHH patterns. In order to determine which of these patterns are (linearly) stable, we perform linear stability analysis on the governing set of nine equations for nine variables for nine cells present in a 3×3 periodic lattice. This procedure, as is well known, yields nine eigenvalues (λ) from the characteristic equation obtained from the set of equations linearized about each of the fixed points (x^*, y^*). A pattern is stable if the maximum of the real parts of the eigenvalues ($\max[\mathrm{Re}(\lambda)]$) is less than zero. In Fig. 9 we see that for additive interaction there is no range of parameters, at least within the values experimented with herein, for which the HLL pattern could be stable. On the contrary, for the multiplicative bidirectional symmetrical repression, only the $\mathcal{H}$ and the HLL patterns can be stable, though not simultaneously. This is in agreement with what has been reported in Ref. [18].

V. THREE-DIMENSIONAL LATTICES

An $L \times L$ bidirectional 2D lattice could be generalized to $L \times L \times L$ 3D lattice without much ado. However, consistent generalization of the unidirectional repressor lattice (or activator-activator-repressor lattice, for that matter) to three dimensions is not possible, as has been explained in Fig. 10. The easiest way to view the 3D bidirectional lattice is to think of layers of cells stacked upon one another forming a close packing structure (tissue): either face-centered cubic structure or hexagonal close-packed structure. Just as in the case of the 2D lattices studied herein, one can find oscillations for the case of the 3D (additive or multiplicative) bidirectional lattice when the mutual repression between two adjacent cells is asymmetrical. When the bidirectional repression is symmetrical, one can find ordered patterns. However, while a homogeneous solution akin to a 2D case is possible, the HLL or the LHH patterns cannot be seen in a 3D lattice just because their constructions are not geometrically possible. Instead, one finds more involved nonhomogeneous stable ordered patterns emerging, as shown in Fig. 11, wherein in the specific case of a $3 \times 3 \times 3$ periodic lattice, seven different equilibrium concentrations are distributed among the cells in an ordered fashion. For completeness, we write below the equation describing the 3D symmetrical bidirectional repressor lattice model:

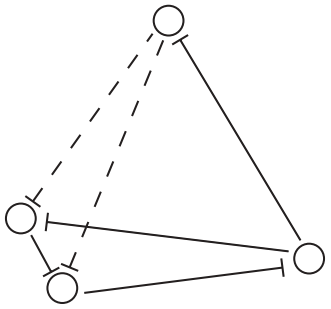

FIG. 10. A typical tetrahedron in the 3D lattice formed by three cells in a particular layer and a fourth cell in the adjacent parallel layer above. One can notice, as highlighted by the dashed lines, all the triplets of adjacent cells in the tetrahedron cannot form repressilators simultaneously. Thus, consistent generalization of the unidirectional repressor lattice to three dimensions is not possible.

$$\frac{dx_{m,n,p}}{dt} = c - \gamma x_{m,n,p} + \alpha F_{\mathrm{int}}; \quad m,n,p \in [1,2,\ldots,L], \tag{21}$$

with

$$\begin{aligned} F_{\mathrm{int}} \equiv & \frac{1}{1 + \left(\frac{x_{m-1,n+1,p}}{K}\right)^h} \circ \frac{1}{1 + \left(\frac{x_{m,n-1,p}}{K}\right)^h} \circ \frac{1}{1 + \left(\frac{x_{m+1,n,p}}{K}\right)^h} \\ & \circ \frac{1}{1 + \left(\frac{x_{m-1,n,p}}{K}\right)^h} \circ \frac{1}{1 + \left(\frac{x_{m,n+1,p}}{K}\right)^h} \circ \frac{1}{1 + \left(\frac{x_{m+1,n-1,p}}{K}\right)^h} \\ & \circ \frac{1}{1 + \left(\frac{x_{m,n,p-1}}{K}\right)^h} \circ \frac{1}{1 + \left(\frac{x_{m+1,n,p-1}}{K}\right)^h} \circ \frac{1}{1 + \left(\frac{x_{m,n+1,p-1}}{K}\right)^h} \\ & \circ \frac{1}{1 + \left(\frac{x_{m,n,p+1}}{K}\right)^h} \circ \frac{1}{1 + \left(\frac{x_{m,n-1,p+1}}{K}\right)^h} \circ \frac{1}{1 + \left(\frac{x_{m-1,n,p+1}}{K}\right)^h}. \end{aligned} \tag{22}$$

Here $x_{m,n,p}$ stands for the concentration/activity of a regulatory protein in cell at coordinate (m,n,p) in the lattice, and the binary operation $\circ$ is $+$ and $\times$, respectively, for the additively and the multiplicatively interacting models. Other symbols are in their usual meanings.

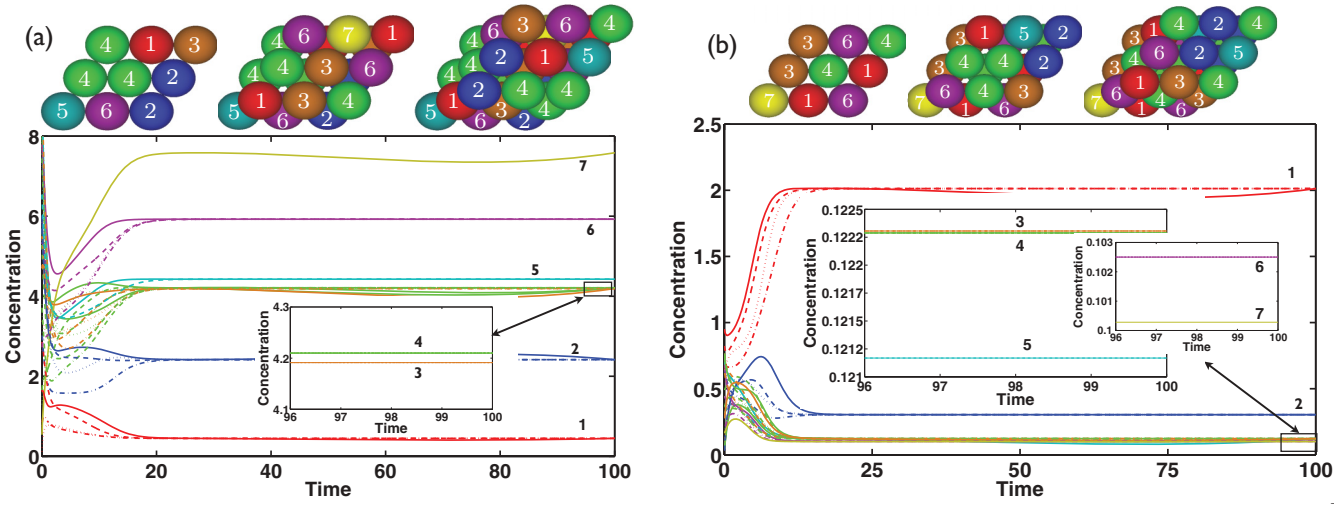

FIG. 11. (Color online) One can see the seven-state patterns in $3 \times 3 \times 3$ periodic symmetrically bidirectional 3D repressor lattice with (a) additive interactions and (b) multiplicative interactions. Seven colors have been used to mark seven different equilibrium concentrations which the different cells settle for. To assist reading in black and white mode, numbers 1 to 7 have been used to tag the equilibrium concentrations. Insets have been provided to zoom into seemingly indistinguishable curves. The schematic patterns, drawn on the top of each of panels (a) and (b), have consistently numbered cells, and they show the seven-state pattern explicitly. Here we have used $c = 0.1$, $\gamma = 1$, $\alpha = 2$, $K = 1$, $h = 3$ [cf. Eq. (21)].

VI. CONCLUSIONS

We have comprehensively extended the study started in Ref. [2] on repressor lattices. Such a lattice presents a simple starting point to study regulation in the spatially extended biological systems. We have primarily investigated (1) a simple case where activators replace systematically some of the repressors in the lattice, (2) cases when feedbacks in repressor lattice are no longer unidirectional but instead bidirectional, and (3) situations when such lattices are 3D. We have presented analytical results, validated numerically, showing how biological oscillations and ordered patterns appear in such systems, and how they may depend on the type of interaction between the cells. All our studies reported herein have been done with periodic boundary conditions. For an extended system with a finite boundary, we expect qualitatively similar behavior in the bulk away from the boundaries.

The limit cycle oscillations of the concentration of the regulatory protein in the cells of the lattice can be seen when only unidirectional or asymmetrically bidirectional repressing feedbacks are present between the neighboring cells, and also when the lattice is the generalization of simple circuit of a negative feedback loop composed by both activators and repressors. As the strength of the nonlinear interaction terms increase, the stable oscillations can in principle become chaotic. When the bidirectional repressing feedbacks in the corresponding lattice are symmetrical, stable patterns emerge: In two-dimensional lattice with symmetric additive bidirectional interaction between cell, a periodic low-high-high pattern is favored, while multiplicative interactions favor a periodic high-low-low pattern. In both the cases, a stable homogeneous state, where all the cells in lattice have the same concentration of the regulatory protein, is also a possibility depending on the relative strength of the nonlinear interaction terms. The 3D generalizations of such lattices give rise to more complex stable patterns where the cells in the lattice take one of the seven different equilibrium concentrations. Extensive investigation on how mutations affect such patterns and how ordered patterns appear during tissue growth, due to the similar cell-to-cell interactions studied in this paper, is reported elsewhere [18].

The results of this paper could provide the starting point for a deeper understanding of the cell-to-cell interactions in ordered tissues. In particular, an investigation of the stability of the ordered patterns could give insights into how possible defects and disorder in the patterns might lead to unhealthy tissues. With our model it is possible to study such effects under a large variation of the different parameters for the cell-to-cell interactions.

ACKNOWLEDGMENTS

This work was supported by the Danish National Research Foundation through the "Center for Models of Life." We thank the anonymous referees for helping us in improving the presentation of this paper.

[1] K. Sneppen, S. Krishna, and S. Semsey, Annu. Rev. Biophys. **39**, 43 (2010).

[2] M. H. Jensen, S. Krishna, and S. Pigolotti, Phys. Rev. Lett. **103**, 118101 (2009).

[3] M. B. Elowitz and S. Leibler, Nature (London) **403**, 335 (2000).

[4] J. Garcia-Ojalvo, M. B. Elowitz, and S. H. Strogatz, Proc. Natl. Acad. Sci. USA **101**, 10955 (2004).

[5] E. Ullner, A. Zaikin, E. I. Volkov, and J. Garcia-Ojalvo, Phys. Rev. Lett. **99**, 148103 (2007); E. Ullner, A. Koseska, J. Kurths, E. I. Volkov, H. Kantz, and J. Garcia-Ojalvo, Phys. Rev. E **78**, 031904 (2008).
[6] J. P. Revel and M. J. Karnovsky, J. Cell Biol. **33**, C7 (1967).
[7] H. Sawada, H. Konomi, and K. Hirosawa, J. Cell Biol. **110**, 219 (1990).
[8] G. Vozzi, A. Previti, D. De Rossi, and A. Ahluwalia, Tissue Eng. **8**, 1089 (2002).
[9] D. Sprinzak, A. Lakhanpal, L. LeBon, L. A. Santat, M. E. Fontes, G. A. Anderson, J. Garcia-Ojalvo, and M. B. Elowitz, Nature (London) **465**, 86 (2010).
[10] S. Artavanis-Tsakonas, K. Matsuno, and M. E. Fortini, Science **268**, 225 (1995).
[11] J. F. de Celis, S. Bray, and A. Garcia-Bellido, Development **124**, 1919 (1997); http://dev.biologists.org/content/124/10/1919.short.
[12] L. Herrgen, S. Ares, L. G. Morelli, C. Schröter, F. Jülicher, and A. C. Oates, Curr. Biol. **20**, 1244 (2010).
[13] M. Tanemura, H. Honda, and A. Yoshida, J. Theor. Biol. **153**, 287 (1991).
[14] H. Honda, M. Tanemura, and S. Imayama, J. Invest. Dermtol. **106**, 312 (1996).
[15] J. R. Collier, N. A. M. Monk, P. K. Mainia, and J. H. Lewis, J. Theor. Biol. **183**, 429 (1996).
[16] S. J. Eglen and D. J. Willshaw, Development **129**, 5399 (2002).
[17] H. Honda and A. Mochizuki, Dev. Dyn. **223**, 180 (2002).
[18] B. Mengel, S. Krishna, S. Chakraborty, S. Pigolotti, V. Sekara, S. Semsey, and M. H. Jensen (unpublished).